Mechanism of Molecular Ordering in Monolayer Liquid Crystal Films

David L. Patrick, Victor J. Cee, and Thomas P. Beebe, Jr.*

Department of Chemistry, The University of Utah, Salt Lake City, Utah 84112

Received: January 26, 1996[⊗]

Scanning tunneling microscopy and "molecule corrals" were used to measure the temperature dependence of the rate of molecular ordering in monolayer liquid crystal films. Molecule corrals are circular etch pits, 3.35 Å deep on the basal surface of graphite formed by high-temperature oxidation. A strong negative relationship between temperature and nucleation rate was observed, consistent with a nucleation growth mechanism of molecular self-assembly. From a fit of classical nucleation theory the melting temperature of the film was found to be $T_{melt} = 318 \pm 6$ K, the thermodynamic driving force for nucleation $\Delta F_n(T_{melt} - T)/T_{melt} = 1.1 \pm 0.3$ kcal mol^{-1}, and the preexeponential factor $A = (1.8 \pm 0.8) \times 10^8$ Å^{-2} s^{-1}.

Introduction

Ordered monolayers of certain liquid crystal molecules have been the subject of extensive investigation since Frommer and co-workers discovered in 1988 that these systems could be studied at molecular length scales with scanning probe microscopy (SPM).[1] Aside from investigations of biological macromolecules, liquid crystal films are probably the most studied molecular system by SPM.[2] It is therefore surprising that although more than two dozen reports have been published describing aspects of these systems ranging from molecular packing structures to grain boundary diffusion, no general description of the mechanism by which molecular order originates in monolayer liquid crystal films has yet been formulated.

In this study we show that molecular ordering in certain liquid crystal films on graphite can be understood in terms of classical nucleation theory (CNT). CNT has been formulated with minor variations and successfully applied to the study of phase transitions in hundreds of systems, from vapor condensation to crystallization from melts. The version of CNT used here is due primarily to Turnbull and Fisher.[3] By demonstrating the applicability of CNT to molecular ordering in liquid crystal films on graphite, experimental results can be interpreted in terms of a rich theoretical framework and connected to a large body of related work.

According to CNT, crystallization proceeds by a two-step process beginning with the formation of nuclei, followed by the growth of ordered molecular domains around those nuclei. It is with the first of these two steps that this paper is concerned. Nuclei are small molecular aggregates of some critical size above which growth is spontaneous. They typically contain 10^2-10^3 molecules.[4] Molecular aggregates smaller than the critical size are called "germs". Full derivations of the equations governing the rate of formation of nuclei have been presented by many authors. We will therefore limit our discussion of the details of nucleation theory and remark only that the nucleation rate J depends on two factors: a kinetic factor related to the rate at which adsorbed molecules diffuse and impinge on the edge of a growing germ and a second factor, ΔF_n, known as the "thermodynamic driving force". The driving force is related to the amount of supersaturation (in the case of a crystal growing from solution) or supercooling (in the case of a crystal growing from the melt). It represents the amount of energy required to generate a nucleus of critical size. As discussed below, the relatively narrow temperature range covered in this study means that the kinetic term related to molecular diffusion remains essentially constant; the changing nucleation rate is due mostly to the thermodynamic driving force.

The phase transition of interest in this report involves the conversion of physisorbed, disordered molecular monolayers to a crystalline phase. We denote these two phases D_{ads} and C_{ads}, respectively. A third bulk smectic-A liquid crystal phase is also present in the form of a covering droplet but is not directly probed in these experiments. Formation of the D_{ads} phase is accomplished by adsorption from the bulk droplet and is virtually instantaneous on the time scale of these experiments. The mechanism of molecular ordering is thus inherently two-dimensional, as it involves the transition between two adsorbed phases $D_{ads} \rightarrow C_{ads}$. Under these conditions, the rate of nucleus formation of the C_{ads} phase is given approximately by

$$J \approx A \exp\left[\frac{-E_d - \Delta F_n}{kT}\right] \tag{1}$$

where E_d is the diffusion energy of an adsorbed molecule, A is a constant, and the free energy of formation of a surface nucleus from the melt (the driving force) is

$$\Delta F_n = \frac{\pi\sigma^2\alpha}{\Delta H_f}\frac{T_{melt}}{T_{melt} - T} \tag{2}$$

The area occupied by a single adsorbed molecule is α, σ is the interfacial energy of the crystal−melt interface, T_{melt} is the melting temperature of an infinitely large 2-D crystal, and ΔH_f is the heat of fusion per molecule. Equation 1 assumes that the nucleus is circular in shape and that growth occurs exclusively through the impingement of adsorbed molecules on the nucleus edge.

That nucleation theory might be applicable to molecular ordering in monolayer films of liquid crystals was suggested by a recent report on the part of the current authors describing measurements of the rate of molecular ordering in these systems.[5] Using "molecule corrals" and SPM (see below), it was determined that (1) there exists a rate-limiting step during the formation of an ordered monolayer which depends on temperature, (2) the rate of this step was very small compared to the rate of domain growth (*i.e.*, once growth initiates it is very rapid, leading to molecular ordering on large regions of the surrounding substrate surface), (3) the characteristic time

* To whom correspondence should be addressed.

⊗ Abstract published in *Advance ACS Abstracts,* April 1, 1996.

S0022-3654(96)00279-1 CCC: $12.00 © 1996 American Chemical Society

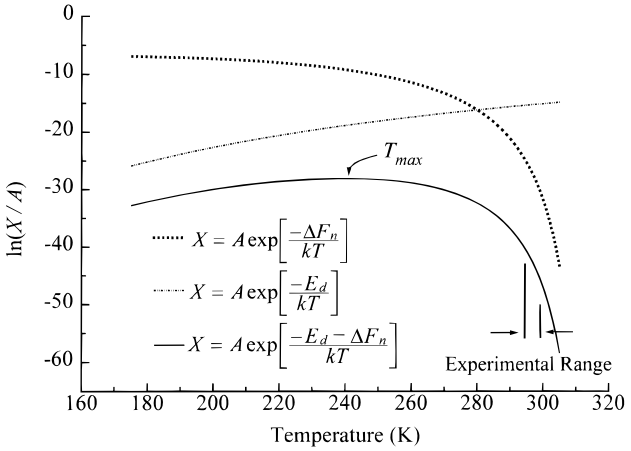

Figure 1. According to classical nucleation theory, the nucleation rate has a complex temperature dependence arising from a competition between kinetic and thermodynamic factors. The plot demonstrates this dependence for the overall normalized nucleation rate (solid line), as well as for each of the two competing factors. (Thickly dotted and thinly dotted lines are contributions from the thermodynamic and kinetic factors, respectively.) The plot was generated based on experimentally determined values of ΔF_n, E_d, and A. For a definition of parameters, refer to text. The temperature corresponding to the maximum nucleation rate T_{max} occurs near 240 K, roughly 70 K below the film melting temperature. Only a relatively narrow range of temperatures is experimentally accessible, as marked by the arrows on the solid line.

of the rate-limiting step is inversely proportional to the amount of substrate surface area not covered by an ordered molecular domain, and (4) molecular ordering occurs independently in each corral.

Viewed in the context of CNT, these observations can be interpreted as follows: (1) The rate-limiting step is associated with the formation of nuclei and should be governed by eq 1. (2) The rate of growth is much greater than the rate of nucleation. (3) Nucleation is homogeneous in the sense that substrate defects such as step edges do not appreciably affect the rate expression. (4) Formation of a separate nucleus is required to initiate molecular ordering in each corral; since molecules in each corral undergo ordering independently from those in all other corrals, separate nucleation events must be occurring. Thus, each of the four principal observations from the previous study outlined above is consistent with and suggestive of a nucleation growth type mechanism.

To further explore whether or not CNT can be applied to ordering in liquid crystal films, we have performed additional measurements of the rate of nucleation as a function of temperature. A distinguishing characteristic of nucleation theory is the prediction that, for moderate amounts of supercooling, there should exist a negative relationship between the nucleation rate and temperature. Thus, over a certain temperature regime, the nucleation rate should *increase* with decreasing temperature.

This trend is illustrated in Figure 1, which shows the temperature dependence of the normalized nucleation rate J in eq 1 (solid line). The values of ΔF_n and E_d used to generate the plot were determined experimentally, as will be discussed below. Note that for moderate amounts of supercooling J increases with decreasing temperature, reaching a maximum a

$$T_{max} = (T_{melt}/E_d)(B + E_d - B^{1/2}(B + E_d)^{1/2})$$

where $B = \pi\sigma^2\alpha/\Delta H_f$. Below this temperature J begins to diminish, eventually reaching zero at zero absolute temperature. This behavior can be viewed as arising from a competition between the two terms in the numerator of the exponent in eq 1. The second term, ΔF_n, acts to increase the nucleation rate

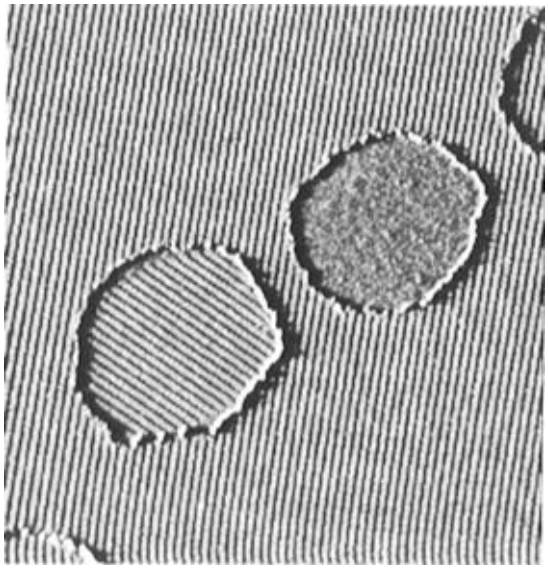

Figure 2. A 3000 × 3000 Å STM current image of two molecule corrals ($V_{bias} = -1.0$ V, $I_{tunn} = 90$ pA, scan rate = 7.34 μm s^{-1}). The figure shows a pixelwise average of five images, individually corrected for drift. Each corral is ~1000 Å in diameter. The rowlike features on the terrace and in one corral arise from an ordered molecular monolayer of liquid crystal molecules (refer to text). At the time this image was acquired, molecular ordering had only occurred in approximately 50% of all corrals. The rate of nucleation in the liquid crystal monolayer was determined by a statistical sampling of corrals in STM images, from which we determine the nucleation rate constant for molecular ordering in the corrals.

with decreasing temperature as the free energy difference between molecules in the melt and crystal phases becomes larger, as is evident from an inspection of the denominator of eq 2. The first term, E_d, is nominally independent of temperature, eventually giving the nucleation rate behavior an Arrhenius-like character at low temperature. The two terms are plotted separately in Figure 1 to illustrate their individual contributions to the overall nucleation rate.

In physical terms, the initial increase in J with reduced temperature arises from the increased thermal stability of the C_{ads} phase over the D_{ads} phase. As the temperature is reduced further, however, the mobility of molecules in the D_{ads} phase begins to decrease, eventually having a negative effect on the nucleation rate. The combination of these conflicting energetic and kinetic factors produces the peaked temperature behavior in Figure 1.

Experimental Section

Nucleation rate measurements were performed using molecule corrals and scanning tunneling microscopy (STM). Molecule corrals are monolayer-deep (3.35 Å), circular etch pits in the basal plane of graphite formed by high-temperature oxidation (see Figure 2). They are used to contain, and to a certain extent, isolate molecules adsorbed in them from molecules adsorbed on the surrounding terrace. The corral size can be controlled by varying the oxidation time and temperature.[6] The corrals used in this study were produced by heating graphite in an open-air tube furnace at 650 °C for 15 min. Five samples were used with corrals ranging in diameter from 925 to 1553 Å. Corral sizes and other experimental details are summarized in Table 1.

The liquid crystal used was 4′-octyl-4-biphenylcarbonitrile (8CB). At the temperature of the experiments 8CB exists only as a bulk smectic-A phase; *i.e.*, no bulk phase transitions occur in the temperature range studied here. It was applied as a neat

TABLE 1: Summary of Measurements for 8CB Monolayer Nucleation in Molecule Corrals[a]

sample	temp (K)	corral diam (Å)	N[b]	k (10^{-4} corral^{-1} s^{-1})	k' (10^{-10} Å^{-2} s^{-1})
A	294.6 ± 0.5	1085 ± 43	26	10.69 ± 0.17	11.56 ± 0.19
B	295.2 ± 0.5	925 ± 75	109	7.92 ± 0.83	11.78 ± 1.24
C	295.4 ± 0.5	1112 ± 77	59	0.89 ± 0.31	0.92 ± 0.31
D	296.7 ± 0.5	1553 ± 63	60	1.08 ± 0.53	0.57 ± 0.28
E	299.1 ± 0.5	1482 ± 120	262	0.10 ± 0.28	0.06 ± 0.16

[a] Quantities are reported as (mean value ± standard deviation). [b] Total number of corrals analyzed.

liquid directly to corral-containing graphite substrates and imaged with STM. 8CB forms highly ordered crystalline domains on graphite from unit cells containing eight molecules each.[1,7] Within each unit cell the molecules are arranged in a head-to-head configuration that results in a mutual cancellation of their dipoles. Unit cells stack together on the surface, producing the rowlike pattern seen both on the terrace and in some of the corrals in Figure 2. Sample temperature was controlled by changing the room temperature and allowing the sample and microscope to equilibrate for several hours before data collection. Room temperature was monitored with a hand-held digital thermocouple. The effectiveness of this method for reliably controlling sample temperature was confirmed with base line studies using a thermocouple attached directly to the sample holder. The relatively large mass of the copper sample block effectively dampens the effect of thermostatic temperature cycling of the room, resulting in a standard deviation of the sample temperature over long periods of less than 0.5 K.

Results and Discussion

Rate measurements were made by applying molecules to a sample with corrals of a given size at time t_0 and observing the length of time required for molecules to order in a statistical sampling of corrals. A typical image used for part of a nucleation rate measurement is shown in Figure 2. At the time this image was taken, molecules in roughly 50% of all corrals had ordered. The fraction of corrals containing ordered molecules F_0 is described by

$$F_0(t) = 1 - e^{-k(t-t_o)}$$

where k is a characteristic rate constant that depends on corral size and sample temperature. The rate constant k is determined by fitting this expression to the experimental data after correcting for finite sampling time. Further details of the rate measurement process are given elsewhere.[5]

Our previous paper on this subject[5] was concerned with understanding the dependence of k on corral size and shape; the objective of this report is to determine the dependence of k on temperature while holding corral size and shape constant. As a practical matter, it is difficult to produce five samples each with identical corral sizes, and this was not attempted. Rather, five samples with roughly similar corral sizes were produced, and the measured nucleation rates were normalized afterward to account for differences in size. Since the rate of nucleation is known to be essentially proportional to corral area rather than perimeter, rate measurements were normalized by dividing each k by the mean area of the set of corrals used to determine them, $k' = k/\pi\langle R\rangle^2$. The quantity k' is the normalized areal rate constant, k is the measured rate constant, and $\langle R\rangle$ is the mean radius of the set of corrals used to determine k. Calculated in this way, the normalized areal rate constants have units of Å^{-2} s^{-1} and are thus independent of corral size. Table 1 summarizes these data.

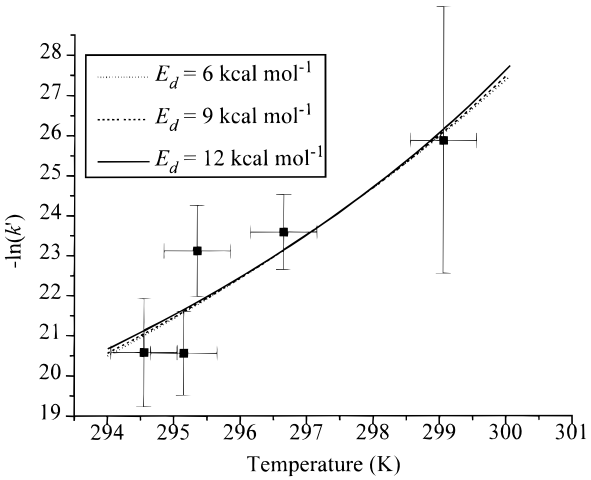

Figure 3. Nucleation rate strongly increases with decreasing temperature. Solid line shows a fit of classical nucleation theory to the experimentally determined normalized rate constants k'.

TABLE 2: Fitted Values[a]

E_d (kcal mol^{-1})	A (10^8 Å^{-2} s^{-1})	ΔF_n ($T_{melt} - T$)/T_{melt} (kcal mol^{-1})	T_{melt} (K)
6	1.7 ± 0.8	1.5 ± 0.4	322 ± 7
9	1.8 ± 0.8	1.1 ± 0.3	318 ± 6
12	1.8 ± 0.8	0.7 ± 0.2	315 ± 5

[a] Quantities are reported as (mean value ± standard error), where the standard error is given by the asymptotic limit of the standard deviation and the square root of the number of measurements $sN^{-1/2}$ as the Marquardt−Levenberg fitting routine used in the minimization converged (Sigma Plot Software, Jandel Corp., 1992).

Figure 3 presents a plot of the normalized rate constant k' against sample temperature for five different temperatures. The temperature range covered, although narrow, is as wide as possible using this technique. At temperatures higher than ~300 K the nucleation rate is so low that several weeks is needed for molecules in a sizable fraction of corrals to order; below ~294 K the rate is too great to measure. Thus, although the temperature range in these experiments was only 4.5 K, the nucleation rate varied by a factor of nearly 200.

In order to fit eq 1 to the data, we estimated the diffusion energy from temperature-programmed desorption experiments (TPD). TPD does not directly measure diffusion energies, and using it to estimate E_d can introduce large uncertainties.[8] Because of this, we fit the data with three different values of E_d, ranging from 6 to 12 kcal mol^{-1}. The value estimated from TPD was E_d = 9 kcal mol^{-1}.

The fitted results are plotted in Figure 3 and summarized in Table 2. The preexponential factor A and melting temperature T_{melt} are fairly insensitive to changes in the estimated diffusion energy, but the thermodynamic driving force changes by a factor of 2 over the range $6 < E_d < 12$ kcal mol^{-1}. Mean-fitted values are $T_{melt} = 318 \pm 6$ K, $\Delta F_n(T_{melt} - T)/T_{melt} = 1.1 \pm 0.3$ kcal mol^{-1}, and $A = (1.8 \pm 0.8) \times 10^8$ Å^{-2} s^{-1}.

Two aspects of the fit to the data in Figure 3 are noteworthy. First, the general trend expected from nucleation theory of a negative relationship between temperature and nucleation rate is reproduced. As stated above, this behavior is consistent with a classical nucleation-type model; the rates of few other surface phenomena *increase* with decreasing temperature. The temperature range covered in these experiments is indicated by arrows in Figure 1 for reference. Using the experimentally determined mean values of ΔF_n, E_d, and A, the temperature corresponding to the maximum nucleation rate was calculated as $T_{max} = 239 \pm 11$ K (see Figure 1).

The second important point is that the fitted value of T_{melt} is consistent with previous STM-based estimates made on similar liquid crystal compounds, which have indicated that the surface layer melts at approximately 10−15 K above the bulk isotropic transition temperature.[9] For 8CB this corresponds to a melting temperature ($C_{ads} \rightarrow D_{ads}$) of $T_{melt} = 323-328$ K, in good agreement with the value of 318 ± 6 K determined here.

An interesting trend observed during the course of these experiments was that the number of domain boundaries per unit area increased slightly with decreasing temperature. Domain boundaries arise when two nuclei form nearly simultaneously on the same graphite terrace. Growing molecular domains centered about each nucleus meet to form a boundary. The observation of grain boundaries in films formed at temperatures above ∼298 K was very uncommon, but below this temperature they were occasionally observed on large graphite terraces.[10] Although they occur too infrequently to make quantitative measurements, their increasing number with decreasing temperature suggests that the rate of domain growth does not increase as rapidly as does the rate of nucleation. Indeed the rate of growth, being primarily a diffusion-limited, activated process (unlike the rate of nucleation, which has a more complex temperature dependence), should decrease with decreasing temperature, in accordance with the trend observed.

Conclusions

CNT has been shown to quantitatively account for the observed trend in the nucleation rate with temperature. By a statistical analysis of STM images of corral-bound monolayers, quantitative nucleation growth parameters were extracted in variable-temperature experiments with STM. The ∼18 K difference between the film melting temperature and the temperature at which molecular ordering occurs is the amount of supercooling necessary for the nucleation rate to become measurable. The principal findings of a previous study[5] were interpreted within the framework of CNT as indicating that nucleation is the rate-limiting step in the formation of an ordered molecular monolayer and that separate nuclei were needed to produce ordering in each corral.

Acknowledgment. This work was supported by the National Science Foundation (NSF-NYI CHE-9357188) and by the Camille & Henry Dreyfus Foundation.

References and Notes

(1) Foster, J. S.; Frommer, J. E. *Nature* **1988**, *333*, 542.

(2) For a recent overview refer to: Smith, D. P. E.; Frommer, J. E. In *STM and SFM in Biology*; Marti, O., Amrein, M., Eds.; Academic Press: New York, 1993.

(3) Turnbull, D.; Fisher, J. C. *J. Chem. Phys*. **1949**, *17*, 71. See also ref 4.

(4) See, for example: Strickland-Constable, R. F. *Kinetics and Mechanism of Crystallization*; Academic Press: New York, 1968.

(5) Patrick, D. L.; Cee, V. J.; Beebe, Jr., T. P. *Science* **1994**, *265*, 231.

(6) Chang, H.; Bard, A. J. *J. Am. Chem. Soc.* **1990**, *112*, 4598. Chu, X.; Schmidt, L. D. *Carbon* **1991**, *29*, 1251.

(7) Patrick, D. L.; Beebe, Jr., T. P. *Langmuir* **1994**, *10*, 298.

(8) The diffusion energy was estimated from TPD measurements of the desorption energy with the approximation $E_d \approx E_{desorption}/4 = 36/4 = 9$ kcal mol^{-1} kcal mol^{-1} (Adamson, A. *Physical Chemistry of Surfaces*; Wiley-Interscience: New York, 1990). Preliminary TPD measurements were performed in UHV on thin films of 8CB prepared by vacuum sublimation from a bulk 8CB source onto a HOPG crystal in a separate vacuum bell jar. The crystal was then transferred into UHV, where the TPD measurements were carried out by monitoring $m/e = 191$, a major 8CB fragment produced during ionization in the mass spectrometer. The temperature for the monolayer desorption peak was 559 ± 11 K, from which a first-order Redhead desorption energy of 35.7 ± 0.8 kcal mol^{-1} was calculated, assuming a preexponential factor of 1013 s^{-1}.

(9) The STM measurements were made by observing the temperature associated with the onset of molecular disorder in the monolayer. Although more direct than the method used here, the direct approach is complicated by the fact that the STM tip and/or electric field may perturb the molecules and alter the measured melting temperature (Spong, J. K.; LaComb, Jr., L. J.; Dovek, M. M.; Frommer, J. E.; Foster, J. S. *J. Phys. (Paris)* **1989**, *50*, 2139).

(10) This fact was exploited in a recent study aimed at understanding the energetics of domain boundaries pinned by substrate defects. In order to generate additional domain boundaries, samples were cooled to 268 K. Under these conditions, up to several boundaries per μm^2 can be observed (Patrick, D. L.; Cee, V. J.; Purcell, T. J.; Beebe, Jr., T. P. *Langmuir*, in press).

JP960279Z